

Supplementary Information

Porous Graphene/CNT@Metal (Hydr)oxide Composite Films Achieving Fast Ion and Electron Kinetics for Asymmetric Supercapacitors with Ultra-High Volumetric Performance

Chunjuan Qiu^a, Baoquan Hou^a, Lili Jiang^{a,}, Huimin Shi^a, Jie Chen^b, Xiaoming Zhou^c,
Xuena Lu^d, Jian Shi^e, Lizhi Sheng^{c,f,*}*

^aKey Laboratory for Special Functional Materials in Jilin Provincial Universities, Jilin Institute of Chemical Technology, Jilin 132022, P. R. China.

^bCenter of Characterization and Analysis, Jilin Institute of Chemical Technology, Jilin 132022, P. R. China.

^cWood Material Science and Engineering Key Laboratory of Jilin Province, Beihua University, Jilin 132013, P. R. China.

^dRiseSun MengGuLi New Energy Science & Technology Co., Ltd., Beijing 102299, P. R. China.

^eHubei Key Laboratory of Low Dimensional Optoelectronic Materials and Devices, Hubei University of Arts and Science, Xiangyang 441053, P. R. China.

^fDepartment of Materials Science and Engineering, National University of Singapore, Singapore 117574, Singapore.

*Corresponding author: jianglidipper@126.com (L. Jiang); shengli_zhi@126.com (L. Sheng).

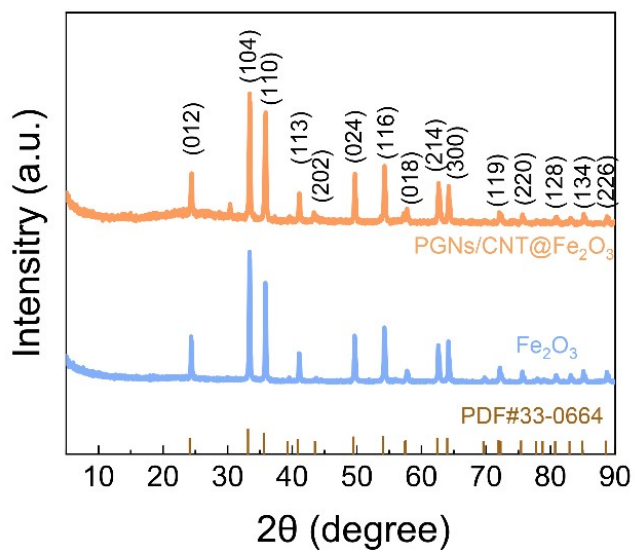


Fig. S1 XRD spectrum of PGNs/CNT@Fe₂O₃ film.



Fig. S2 Physical image of PGNs/CNT@Fe₂O₃ film under bending.

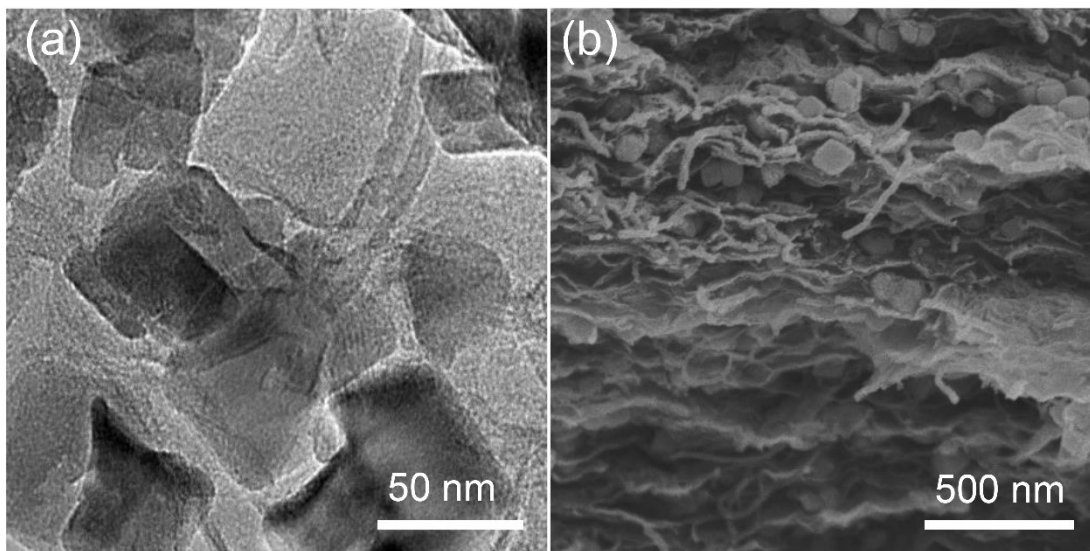


Fig. S3 (a) TEM and (b) SEM image of the PGNs/CNT@Fe₂O₃ film.

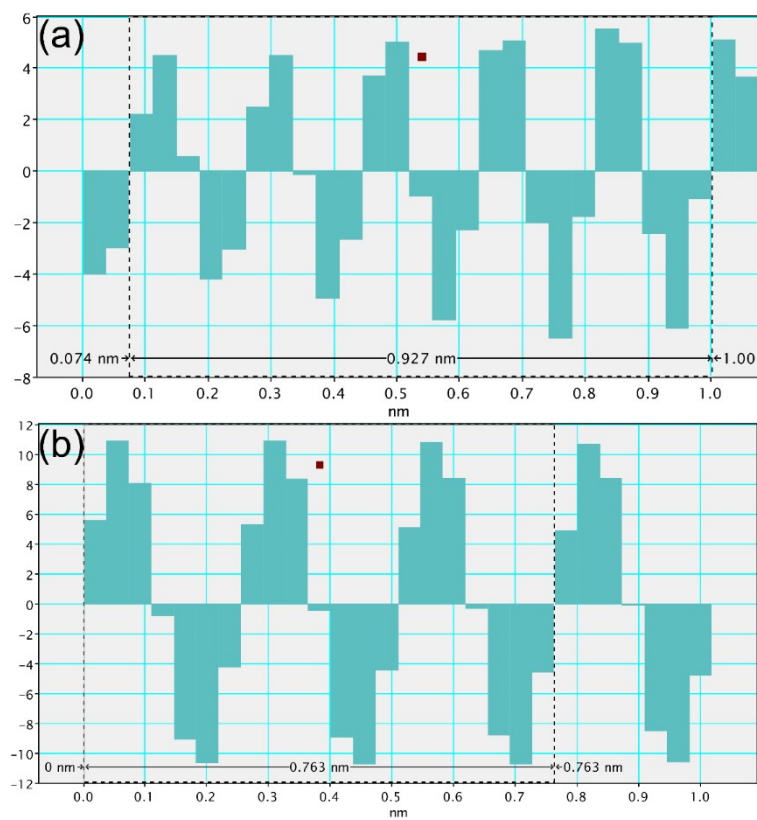


Fig. S4 (a, b) Lattice spacing diagram of PGNs/CNT@Fe₂O₃ film.

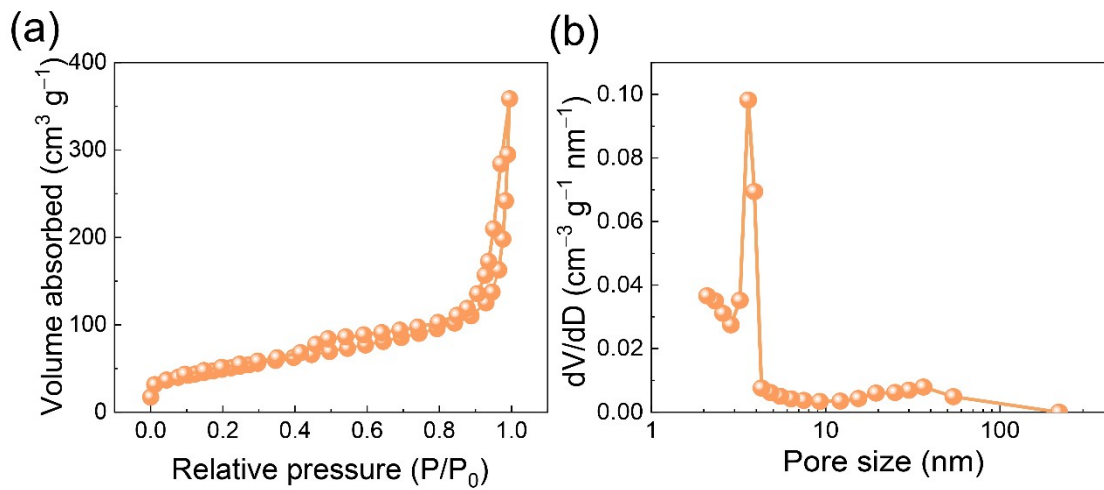


Fig. S5 (a) N₂ adsorption/desorption isotherms and (b) pore-size distribution curves of PGNs/CNT@Fe₂O₃ film.

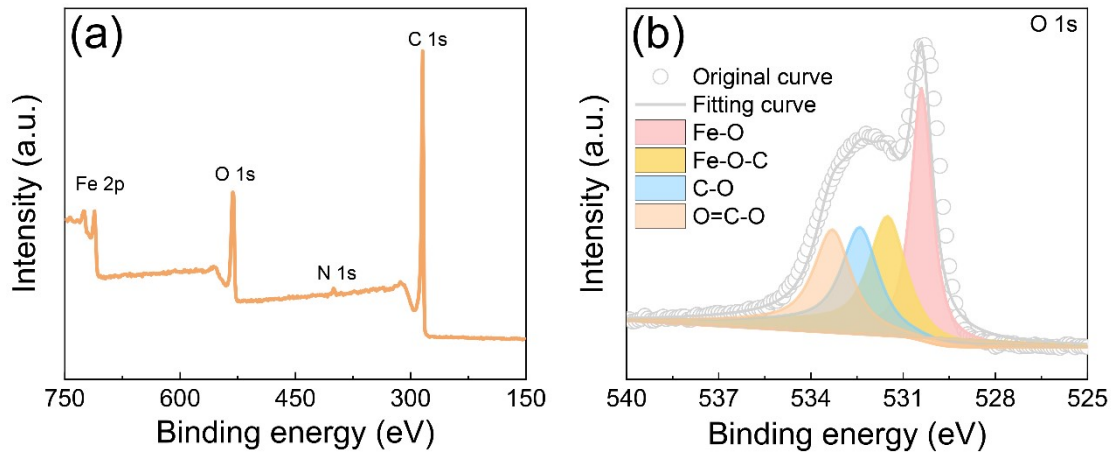


Fig. S6 (a) XPS spectrum of PGNs/CNT@Fe₂O₃ film. (b) O 1s high-resolution XPS spectra of PGNs/CNT@Fe₂O₃ film.

Table S1. The chemical composition of PGNs/CNT@Fe₂O₃ film.

Sample	C 1s At.%	O 1s At.%	N 1s At.%	Fe 1s At.%
PGNs/CNT@Fe ₂ O ₃	79.71	15.06	1.25	3.98

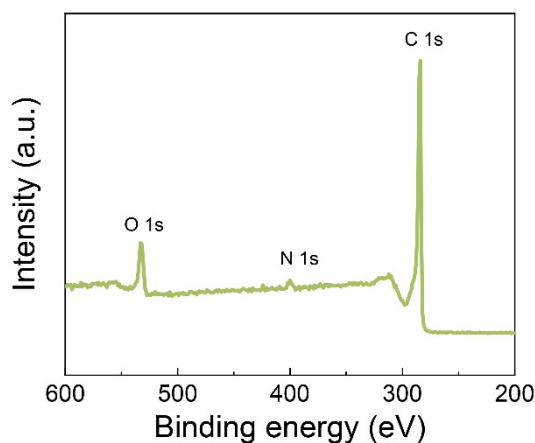


Fig. S7 N 1s high-resolution XPS spectra of PGNs.

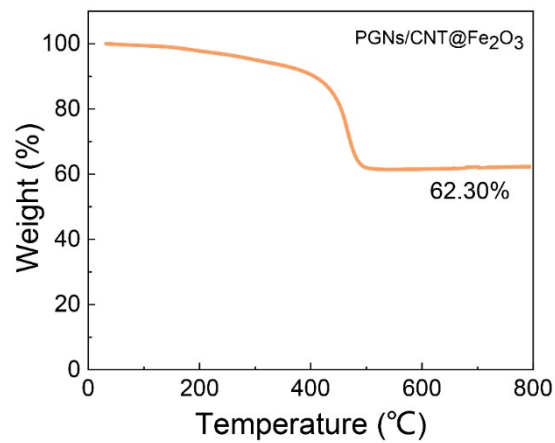


Fig. S8 Thermogravimetric spectra of PGNs/CNT@Fe₂O₃ film.

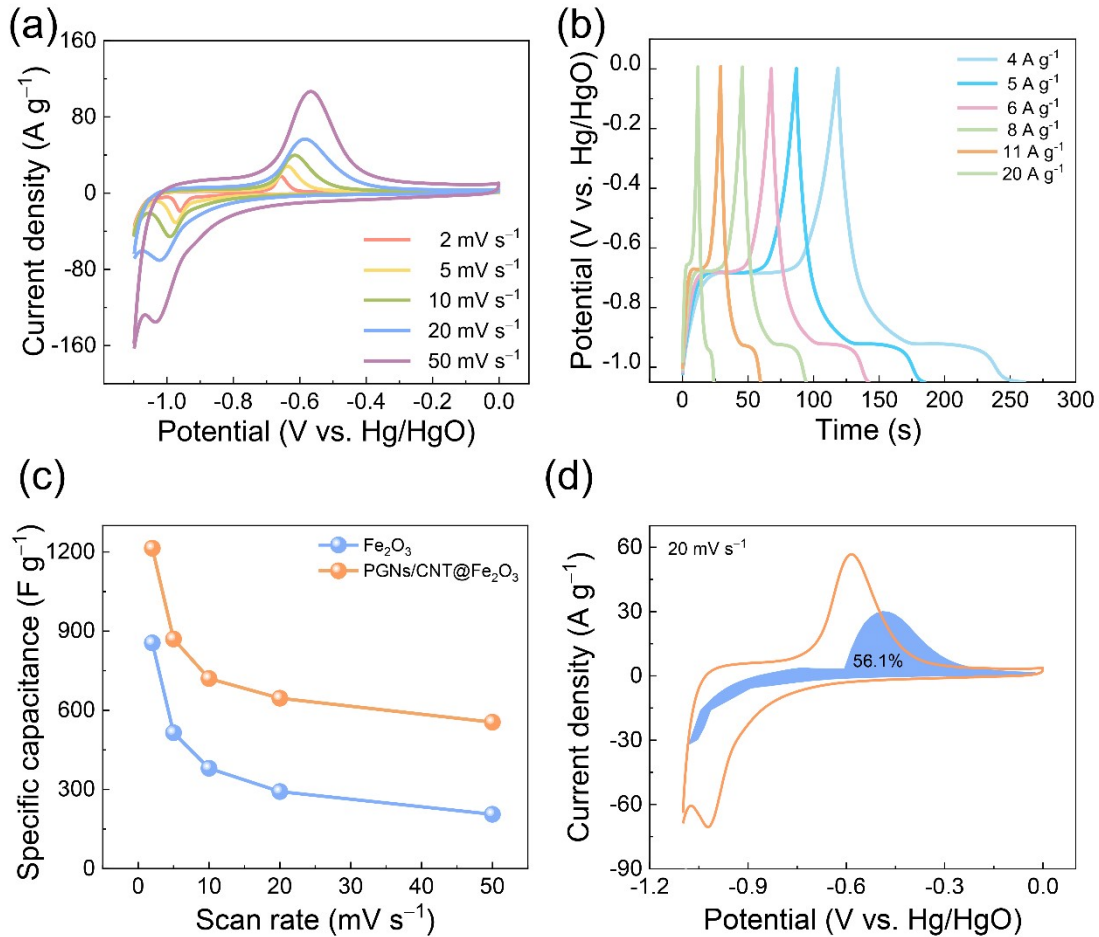


Fig. S9 (a) CV and (b) GCD of PGNs/CNT@ Fe_2O_3 film. (c) Gravimetric capacitance of Fe_2O_3 and PGNs/CNT@ Fe_2O_3 film. (d) PGNs/CNT@ Fe_2O_3 at 20 mV s^{-1} with $k_1 v$ outlined into red area based on $i(V)=k_1 v + k_2 v^{1/2}$.

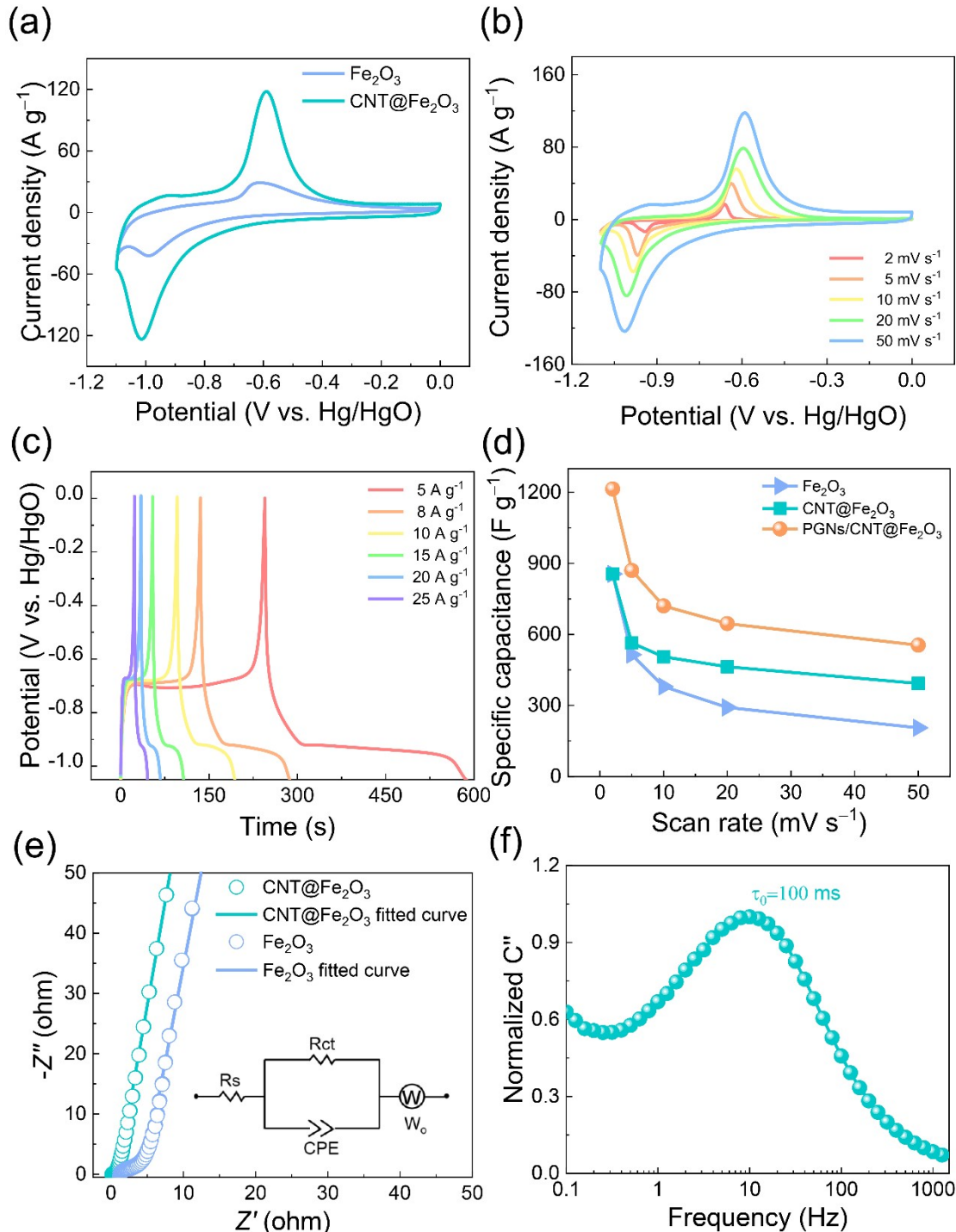


Fig. S10 (a) At 50 mV s^{-1} , the CV curves of Fe_2O_3 and PGNs/CNT@ Fe_2O_3 film. (b) CV curve and (c) GCD curve of $\text{CNT}@\text{Fe}_2\text{O}_3$. (d) Gravimetric capacitance of Fe_2O_3 , $\text{CNT}@\text{Fe}_2\text{O}_3$ and PGNs/CNT@ Fe_2O_3 film. (e) Nyquist plots of Fe_2O_3 and $\text{CNT}@\text{Fe}_2\text{O}_3$ film. (f) τ_0 (ms) of $\text{CNT}@\text{Fe}_2\text{O}_3$.

Table S2 The R_s and R_{ct} of PGNs/CNT@Fe₂O₃, CNT@Fe₂O₃ and Fe₂O₃ fitted through an equivalent circuit.

Sample	R_s (Ω)	R_{ct} (Ω)
PGNs/CNT@Fe ₂ O ₃	0.033	0.29
CNT@Fe ₂ O ₃	0.16	0.06
Fe ₂ O ₃	1.2	1.5

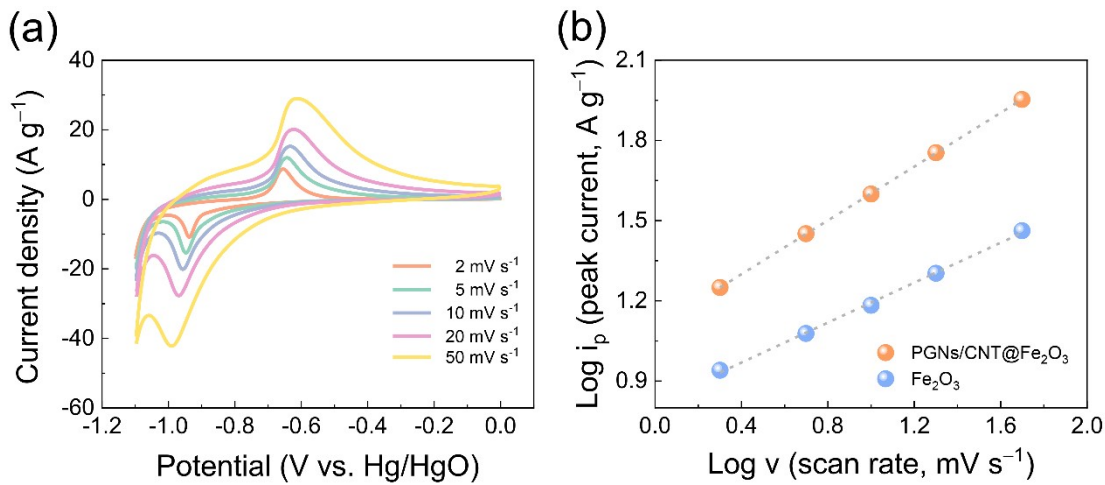


Fig. S11 (a) CV and (b) Power law dependence of log current on log scan rate of Fe₂O₃.

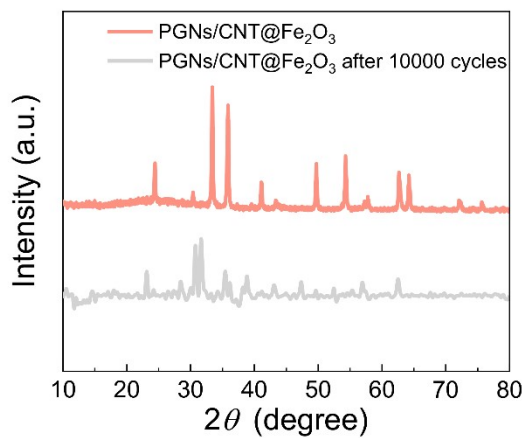


Fig. S12 XRD patterns of PGNs/CNT@Fe₂O₃ film before and after 10,000 cycles.

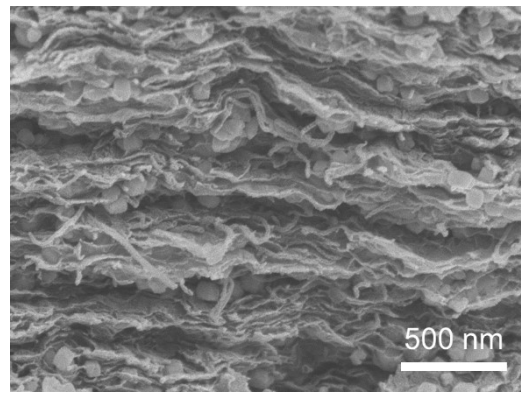


Fig. S13 Cross-sectional SEM image of the PGNs/CNT@Fe₂O₃ film after 10000 cycles.

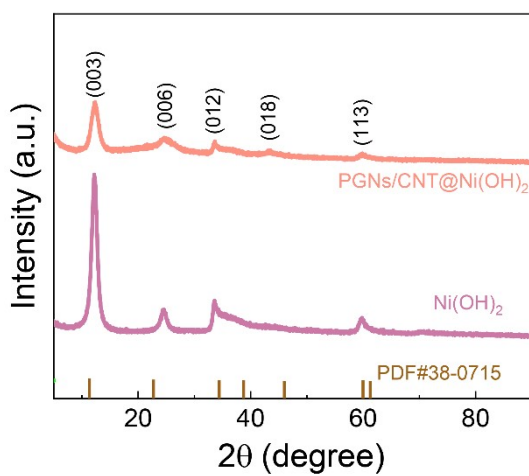


Fig. S14 XRD spectrum of PGNs/CNT@Ni(OH)₂ film.

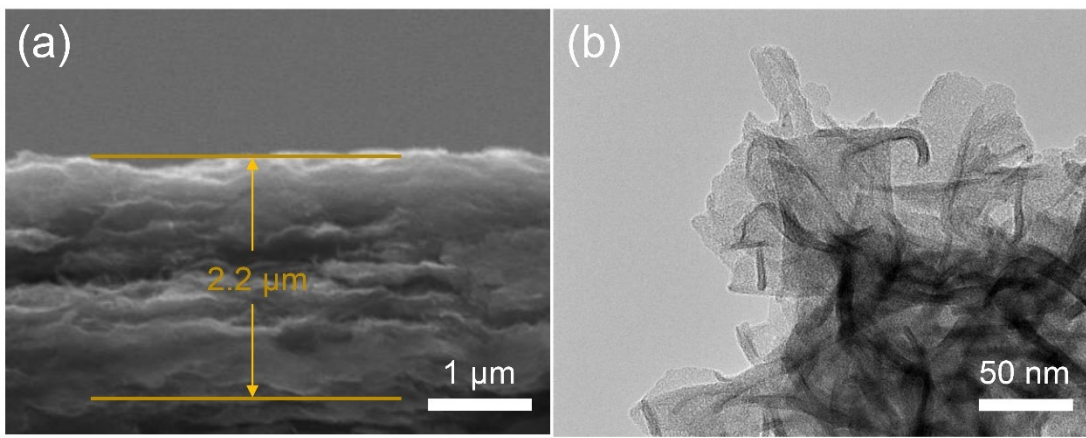


Fig. S15 (a) SEM and (b) TEM image of the PGNs/CNT@Ni(OH)₂ film.

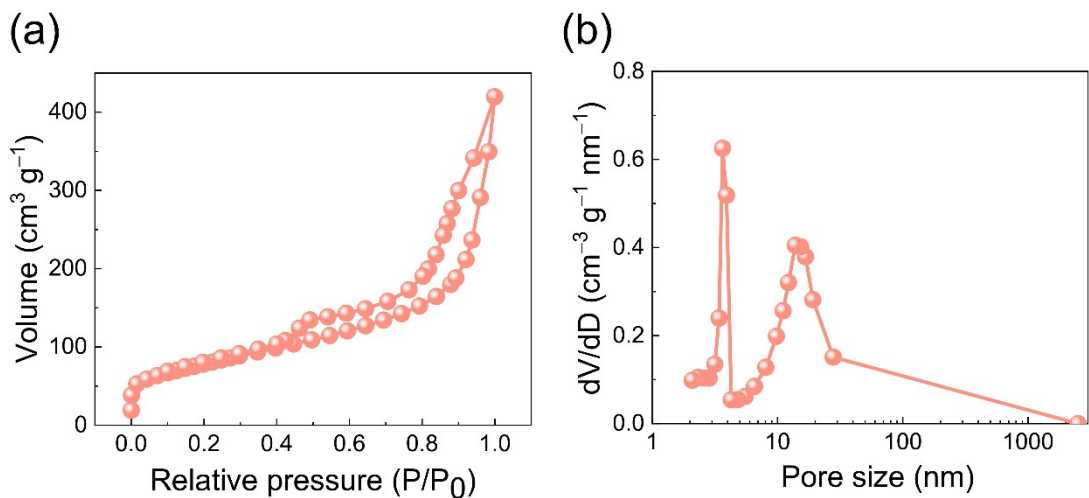


Fig. S16 (a) N_2 adsorption/desorption isotherms and (b) pore-size distribution curves of PGNs/CNT@Ni(OH)₂ film.

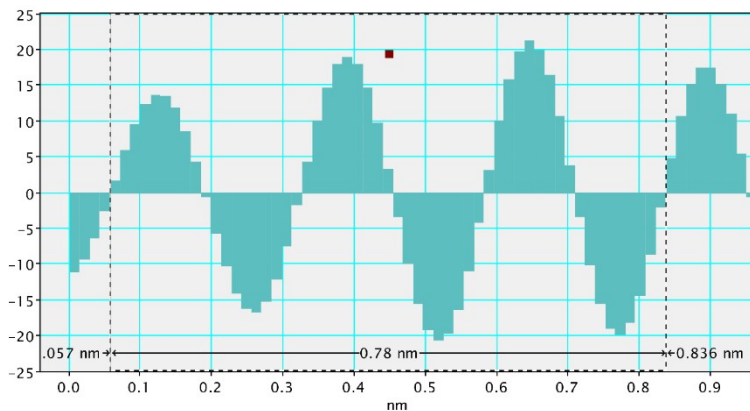


Fig. S17 Lattice spacing diagram of PGNs/CNT@Ni(OH)₂ film.

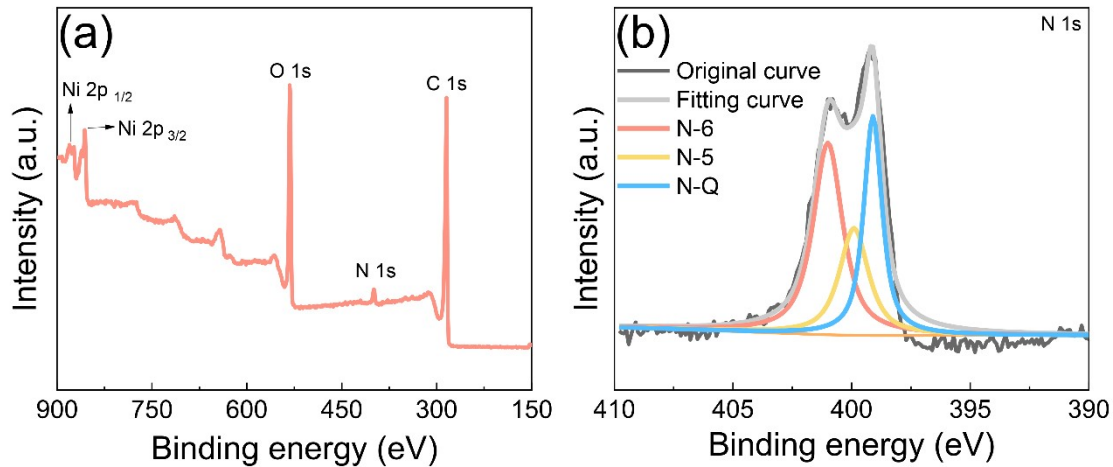


Fig. S18 (a) XPS spectrum of PGNs/CNT@Ni(OH)₂ film. (b) N 1s high-resolution XPS spectra of PGNs/CNT@Ni(OH)₂ film.

Table S3. The chemical composition of PGNs/CNT@Ni(OH)₂ film.

Sample	C 1s At.%	O 1s At.%	N 1s At.%	Ni 1s At.%
PGNs/CNT@Ni(OH) ₂	71.56	21.38	2.68	4.37

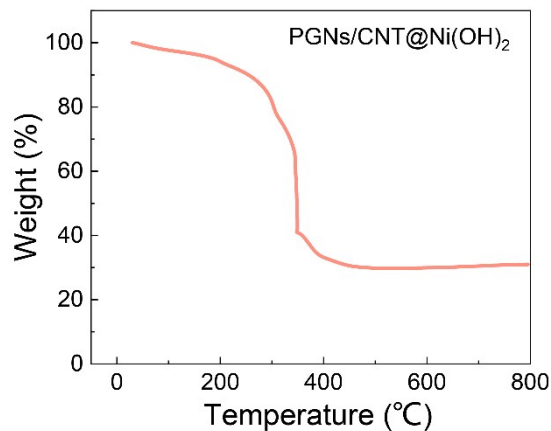


Fig. S19 Thermogravimetric spectra of PGNs/CNT@Ni(OH)₂ film.

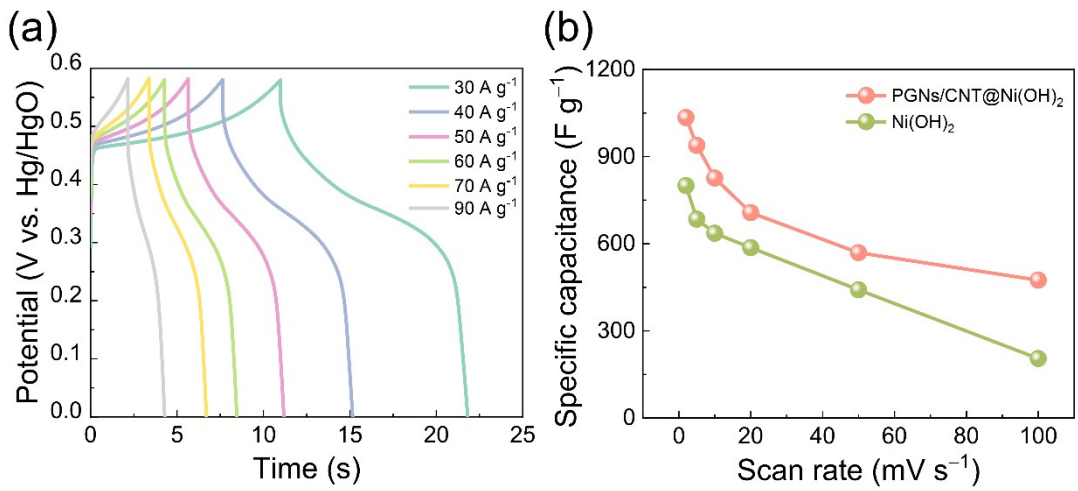


Fig. S20 (a) GCD curves of PGNs/CNT@Ni(OH)₂. (b) The gravimetric capacitance of Ni(OH)₂ and PGNs/CNT@Ni(OH)₂.

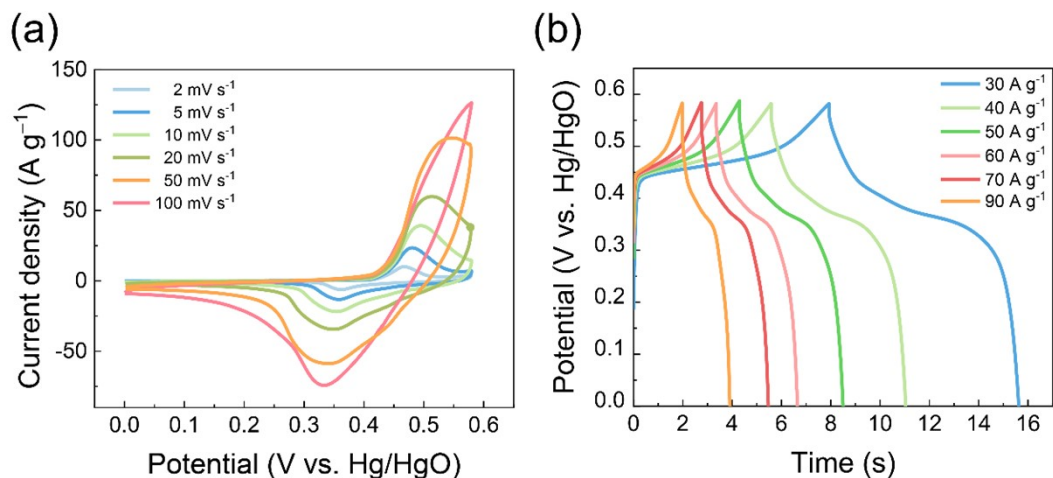


Fig. S21 (a) CV and (b) GCD curves of Ni(OH)₂.

Table S4 The R_s and R_{ct} of PGNs/CNT@ Ni(OH)₂ film and Ni(OH)₂ fitted through an equivalent circuit.

Sample	R_s	R_{ct}
PGNs/CNT@Ni(OH) ₂	0.05	0.59
Ni(OH) ₂	0.1	1

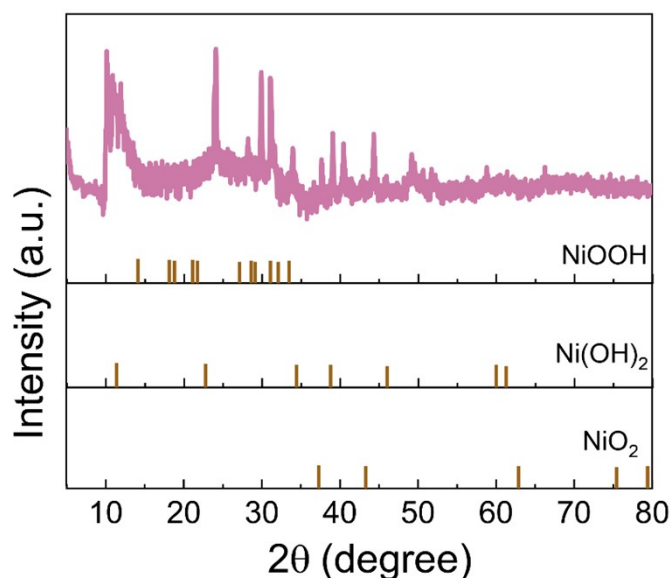


Fig. S22. The XRD test of PGNs/CNT@Ni(OH)₂ after cycling.

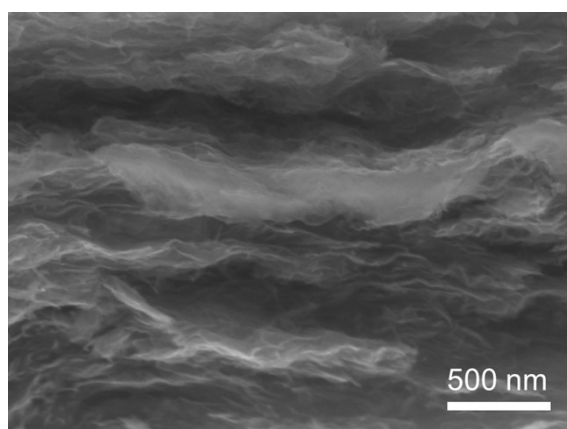


Fig. S23 Cross-sectional SEM image of the PGNs/CNT@Ni(OH)₂ film after 10000 cycles.

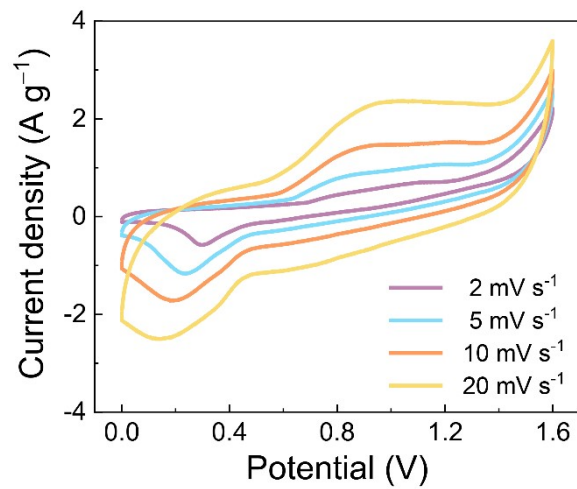


Fig. S24 (a) CV curves of PGNs/CNT@Ni(OH)₂//PGNs/CNT@Fe₂O₃ ASC.

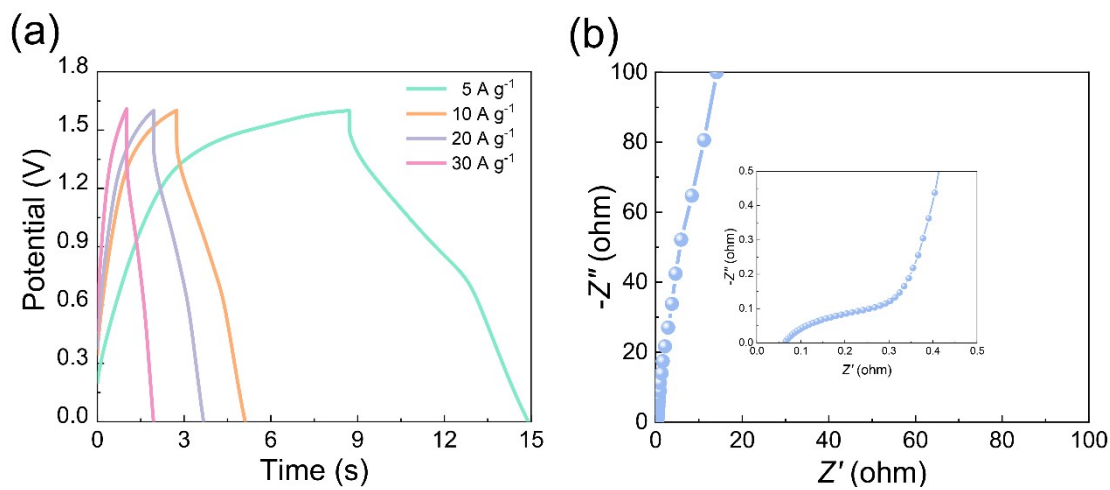


Fig. S25 (a) GCD curves and (b) Nyquist plots of
PGNs/CNT@Ni(OH)₂//PGNs/CNT@Fe₂O₃ ASC.

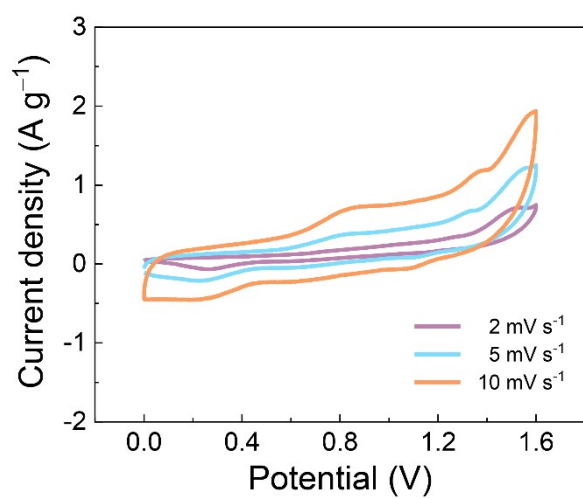


Fig. S26 CV curves of all-solid-state PGNs/CNT@ Ni(OH)_2 //PGNs/CNT@ Fe_2O_3

ASC.